J Mater Sci: Mater Electron (2016) 27:2175–2182
DOI 10.1007/s10854-015-4084-y

REVIEW

Rietveld analysis of $CaCu_3Ti_4O_{12}$ thin films obtained by RF-sputtering

C. R. Foschini[1] · R. Tararam[2] · A. Z. Simões[3] · L. S. Rocha[3] · C. O. P. Santos[2] · E. Longo[2] · J. A. Varela[2]

Received: 8 August 2015 / Accepted: 15 November 2015 / Published online: 25 November 2015

Abstract Calcium copper titanate, $CaCu_3Ti_4O_{12}$, CCTO, thin films with polycrystalline nature have been deposited by RF sputtering on Pt/Ti/SiO_2/Si (100) substrates at a room temperature followed by annealing at 600 °C for 2 h in a conventional furnace. The crystalline structure and the surface morphology of the films were markedly affected by the growth conditions. Rietveld analysis reveal a CCTO film with 100 % pure perovskite belonging to a space group Im3 and pseudo-cubic structure. The XPS spectroscopy reveal that the in a reducing N_2 atmosphere a lower Cu/Ca and Ti/Ca ratio were detected, while the O_2 treatment led to an excess of Cu, due to Cu segregation of the surface forming copper oxide crystals. The film present frequency -independent dielectric properties in the temperature range evaluated, which is similar to those properties obtained in single-crystal or epitaxial thin films. The room temperature dielectric constant of the 600-nm-thick CCTO films annealed at 600 °C at 1 kHz was found to be 70. The leakage current of the MFS capacitor structure was governed by the Schottky barrier conduction mechanism and the leakage current density was lower than 10^{-7} A/cm^2 at a 1.0 V. The current–voltage measurements on MFS capacitors established good switching characteristics.

✉ A. Z. Simões
alezipo@yahoo.com

[1] Dept. de Eng. Mecânica, Faculdade de Engenharia de Bauru, Universidade Estadual Paulista – UNESP, Av. Eng. Luiz Edmundo C. Coube 14-01, Bauru, SP CEP 17033-360, Brazil

[2] Instituto de Química, Universidade Estadual Paulista – UNESP, Rua Prof. Francisco Degni no 55, Araraquara, SP CEP 14800-900, Brazil

[3] Faculdade de Engenharia de Guaratinguetá, Universidade Estadual Paulista – UNESP, Av. Dr. Ariberto Pereira da Cunha, no 333, Guaratinguetá, SP CEP 12516-410, Brazil

1 Introduction

Perovskite-type material $CaCu_3Ti_4O_{12}$ (CCTO) has attracted much attention because of its extraordinarily high dielectric constant (up to 10^4 for bulk ceramic or single crystal) over a broad temperature range [1–9]. With the help of neutron powder diffraction [2] and high-resolution X-ray diffraction (XRD) [3], there is no evidence of any lattice distortion in CCTO from 100 K to 600 K, which is very desirable for practical application in capacitors. In order to apply CCTO in microelectronic devices and give a more fundamental understanding of its physical properties, some groups have grown high-quality epitaxial CCTO films on oxide substrates [10, 11]. The films show single crystalline structure and the dielectric constants are larger than 1500 in a wide temperature region. Recently, we have deposited polycrystalline CCTO thin films with different thicknesses on Pt/Ti/SiO_2/Si substrates [12], and found that the dielectric properties of the polycrystalline CCTO thin films are comparable with those observed in the CCTO films grown on oxide substrates. It is well known that the bottom electrode plays an important role during the fabrication of dielectric or ferroelectric thin films. The electrode materials are required to have certain properties, such as high metallic conductivity, sufficient resistance against oxidation and good adhesion to the films. Therefore, platinum, one of the few metals that satisfy these requirements, has been used as a bottom electrode in high dielectric constant thin-film capacitors [13]. Most of works have been reported on the preparation of CCTO thin films based on physical deposition techniques as pulsed-laser deposition (PLD) [14–16].

The fabrication of sputtered CCTO porous films with high gas sensitivity has been recently reported by Rothschild and Kim et al. [17, 18]. It has been shown that,

depending on the synthesis method and experimental conditions, *n* or *p* type conductivity can be attained [19]. In this paper, we report the growth and electrical and dielectric characterization of CCTO thin films deposited on $Pt/TiO_2/SiO_2/Si$ substrates by RF sputtering without any buffer layer, focusing on potential application in resistive-switching devices.

2 Experimental procedure

The CCTO targets were prepared by conventional solid state reaction. Calcium carbonate, copper oxide and titanium dioxide (>99 % purity and <1 μm) were mixed by ball milling in ethanol for 12 h. After dried the powder was calcined at 900 °C for 12 h. The calcined powder was mixed with PVA as a binder and uniaxially pressed into discs of approximately 50 mm in diameter and 3 mm thickness and sintered at 1100 °C for 3 h. From these targets nanostructured $CaCu_3Ti_4O_{12}$ films deposited on $Pt/Ti/SiO_2/Si$ substrates were obtained by RF sputtering at room temperature in ambient atmosphere. The target substrate distance was kept at 85 mm and temperature, atmosphere and deposition rate were controlled. The Ar deposition pressure was 50 mtorr with 150 W RF power. CCTO films were characterized by X-ray diffraction (XRD, Rigaku, Model Rint 2000) at 40 kV and 150 mA from 2θ (20°–80°) following the phase evolution. The Rietveld analysis was performed with the Rietveld refinement program DBWS-941 1 [20]. The profile function used was the modified Thompson-Cox-Hastings pseudo-Voigt where η (the lorentzian fraction of the function) varies with the Gauss and Lorentz components of the full width at half maximum. The thickness of the annealed films was analyzed using a field emission gun scanning electron microscope (FEG-SEM, JEOL, Model 7500F). Atomic Force Microscopy technique was used to analyze the surface of the films (AFM, NanoScopeIIIa, Bruker). The XPS analysis was carried out at a pressure of $<10^{-7}$ Pa using a commercial spectrometer (UNI-SPECS UHV) to verify the changes in surface chemical composition of the treated specimens. The Mg K line was used (h = 1253.6 eV) and the analyzer pass energy was set to 10 eV. The inelastic background of the Cu 2p, Ca 2p, Ti 2p and O 1 s electron core-level spectra were subtracted using Shirley's method. The composition of the near surface region was determined with an accuracy of ±10 % from the ratio of the relative peak areas corrected by Scofield's sensitivity factors of the corresponding elements. The spectra were fitted without placing constraints using multiple Voigt profiles. The width at half maximum (FWHM) varied between 1.2 and 2.1 eV and the accuracy of the peak position was ±0.1 eV. For electrical DC and AC measurements, top Au electrodes (diameter: 200 μm) were deposited by sputtering through a shadow mask at room temperature acquiring a metal–semiconductor-metal (MSM) capacitor configuration. In DC measurement the current–voltage characteristic was determined with an amperimeter (model- *Keithley 6430)* with a current compliance of 6 μA. The dielectric permittivity (ε) and the dissipation factor (tan δ) were obtained by impedance spectroscopy measurements in the frequency range from 100 Hz to 10 MHz by employing a frequency response analyzer (HP, Model 4192A). All measurements were performed at room temperature.

3 Results and discussion

Figure 1 shows the XRD patterns of stoichiometric CCTO thin films deposited on $Pt/Ti/SiO_2/Si$ substrates and annealed at 600 °C for 2 h in ambient atmosphere. According to the XRD pattern, all XRD peaks can be indexed to $CaCu_3Ti_4O_{12}$. The characteristic peaks of Pt substrate can also be observed in the pattern. CCTO has a cubic structure with lattice parameter $a = 7.379 \pm 0.001$ Å. This is slightly less than the lattice parameter of CCTO reported previously [21]. This shows that the CCTO films can be prepared by the present process at much lower temperature than the solid state ceramic method. The lack of the peak at 49° can be explained by the low surface energy of the peak in the plane (004) due to its strain imposed by the cubic platinum substrate in the plane (111). This indicates that the as-prepared thin film is (h00)-oriented CCTO films. Compared with the XRD intensity from the substrate, the intensity of the XRD reflections from

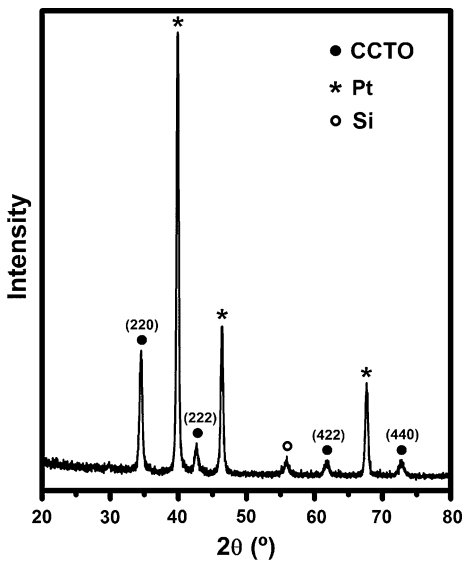

Fig. 1 X-ray diffraction data for CCTO thin film deposited by RF sputtering at room temperature and annealed at 600 °C for 2 h in a conventional furnace

CCTO is obviously smaller. This is mainly due to the polycrystalline character as well as the relatively small thickness of the CCTO films.

In this study, the Rietveld refinement was used to investigate the crystal structure of the CCTO (see Fig. 2a, b). Data were collected from the film annealing at 600 °C for 2 h in a conventional furnace. Figure 2a illustrates the experimental, calculated and difference patterns for the Rietveld refinement of room temperature indexed as representation of the crystal structure of CCTO, Fig. 2b. Crystal structure of the CCTO was used as a tool for structural refinement. In the vertices of the network or corners, half of the inner edges and interior of the octahedra are, respectively, Ca, Cu and Ti. Oxygen elemnt is present in the corners of the octahedra. The main diffraction peaks observed corresponds only to CCTO (JCPDF 75-2188 card). The simulated diffraction refinement and the difference between the experimental data indicate a good structural adjustment, as in agreement with many papers present in literature [22–41] literature. 100 % of perovskite CCTO phase is obtained only when the ratio of calcium, copper and titanium are close to stoichiometric. No evidence of the presence of secondary phases or crystallographic symmetry lowering was found; neither reflection splitting nor superlattice reflections were observed. The refined atomic coordinates, atomic displacement parameters (ADPs) and relevant interatomic distances are summarized below. The relatively high values of the profile R-factors reflect primarily the high statistics of the data; consistently, the Le Bail fit with identical values of profile coefficients yielded a space group Im3, a = 7.39612(3) Å, Z = 2, $\chi^2 = 2.64$, $R_p = 12.0$ %, $R_{wp} = 16.5$ %, $R_B = 4.35$ %, $R_F = 3.84$ %. Refinement was limited to isotropic ADPs: anisotropic refinement did not yield any significant improvement in the fit quality and components of ADP tensors refined with large uncertainties. Fractional coordinates, isotropic ADPs (Biso) and selected interatomic distances (Å) refined by the Rietveld method for the $CaCu_3Ti_4O_{12}$ sample. The absence of byproducts such as $CaTiO_3$ and TiO_2 indicates that no excess titanium in the preparation. Although the presence of CuO has been attributed in some cases to precipitation of $CaTiO_3$, this explanation cannot be validated in this case. It is more likely that a representative amount of CuO has precipitated throughout the preparation process. The non-presence of TiO_2 and $CaTiO_3$ can be attributed, in part, to the use of the selected titanium source material, i.e., titanium dioxide. Other factors that should be influencing the quality of CCTO herein are obtained the purity of raw precursors, and the temperature and time of homogenization of solutions, among others. The results obtained confirmed that the CCTO film crystallized in the pseudo-cubic phase with no changes during the refinement. From the low S values ($S = R_{wp}/R_{exp} = 1.4$ %) it can be assumed that the refinement of the CCTO phase was successfully performed with all the investigated parameters close to literature data.

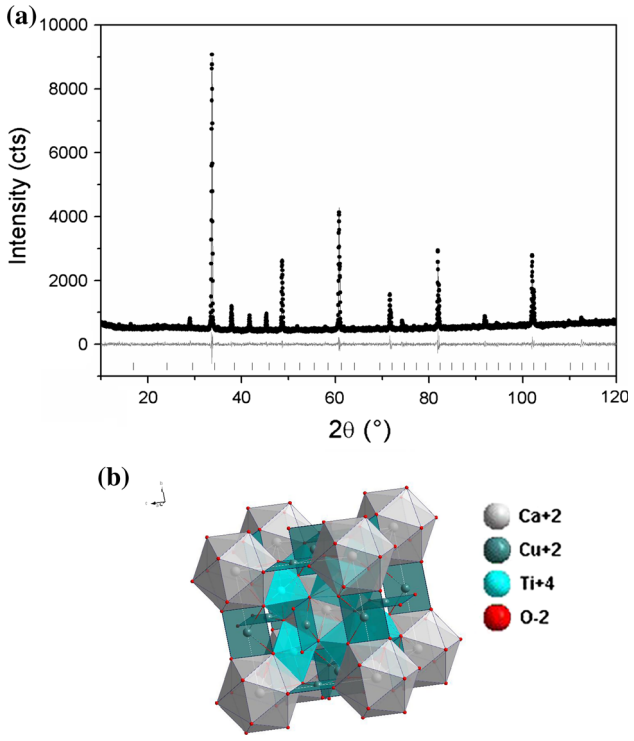

Fig. 2 **a** Rietveld plot and **b** crystal structure for CCTO thin film deposited at room temperature and annealed at 600 °C for 2 h in a conventional furnace

In order to study the interface structure of the CCTO film, the cross sectional SEM image was taken (Fig. 3). As can be seen, there is sharp interface between the CCTO films and the substrate. The thickness of the CCTO film is about 600 nm. It is noted that the CCTO film consists of several grain layers. In the first layer the grains align neatly, suggesting the solid-phase mechanism for the film growth. Though the other layers show random-like assembly of grains, the resultant surface is rather flat. The film shows good adhesion to the substrate and consist of homogeneous and crack-free microstructures formed of interconnected nanoparticles. The grains, are equiaxial, exhibiting uniform sizes (approximately 13 nm). The majority of pores are in the nanoscale range with size of 5 nm, though larger pores (10 nm) could also be observed. The surface morphology of the CCTO thin film was also observed by AFM measurements. CCTO film exhibited homogeneous microstructure consisting of small and large grains with a statistical roughness, root mean square (RMS) of 3.2 nm approximately. The single layer CCTO film formed on Pt/Ti/SiO_2/Si substrates was found to be effective in improving the surface morphology of synthesized film, because the precursor film underwent the optimized

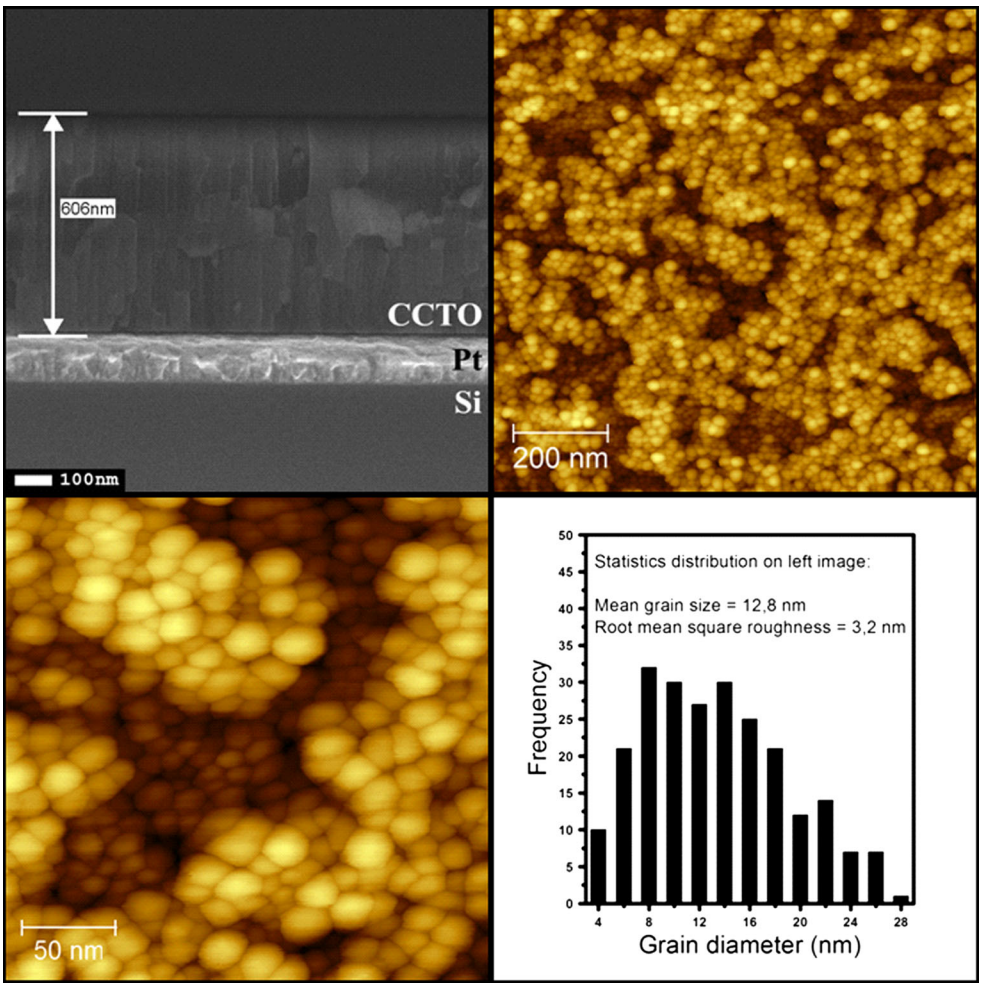

Fig. 3 Cross sectional SEM image and Atomic Force Microscopy for CCTO thin film deposited at room temperature and annealed at 600 °C for 2 h in a conventional furnace

nucleation and growth process producing films with a homogeneous and dense microstructure. Also, the homogeneous microstructure of CCTO film may affect the leakage properties, because the voltage can be applied uniformly onto it. The AFM surface image supports the XRD results revealing the polycrystalline nature.

The XPS spectroscopy provided information on the bonding structure and composition of the near surface region of the material. The results of the quantitative analysis obtained for the as grown reference and samples prepared in oxygen and nitrogen atmosphere are listed in Table 1. Except the lower Ti content, the composition of the reference sample is close to the nominal stoichiometry of $CaCu_3Ti_4O_{12}$. In the case of the reducing N_2 atmosphere a lower Cu/Ca and Ti/Ca ratio were detected, while the O_2 treatment led to an excess of Cu, due to Cu segregation o the surface forming copper oxide crystals. To get a better insight on the processes occurring on the surface, the evolution of the structural components was analyzed by the deconvolution of the Cu $2p_{3/2}$,Ti $2p_{3/2}$ and Ca 2p spectra. The high-resolution Cu $2p_{3/2}$ spectra, displayed in Fig. 4c, show three distinct surface species, which were attributed

Table 1 Atomic concentrations of CCTO RF samples treated in oxygen and nitrogen atmosphere

Element	Concentration (at. %)[a]		
	CCTO RF	CCTO RF-O_2	CCTO RF-N_2
Ca	5.3	4.9	7.1
Cu	14.1	20.4	13.2
Ti	14.3	12.3	15.4
O	66.2	61.1	62.5
S	-[b]	1.3	1.8

[a] Estimated error: ±10 %

[b] Below the detection limit

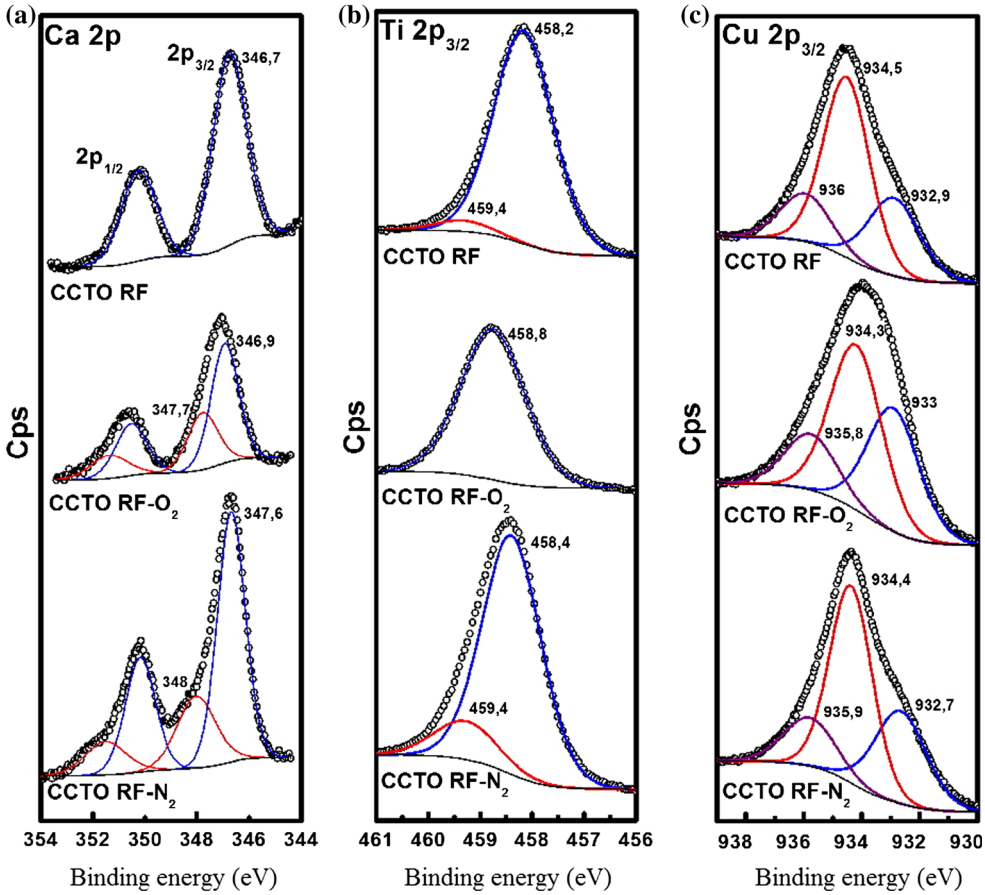

Fig. 4 XPS spectra for CCTO thin film deposited by the RF sputtering at room temperature and annealed at 600 °C for 2 h in a conventional furnace showing: **a** spin orbit doublets of Ca $2p_{3/2}$ and Ca $2p_{1/2}$, **b** Cu $2p_{3/2}$ and **c** Ti $2p_{3/2}$

to $CuCO_3$ (935.9 eV), CuO (934.4 eV) and Cu_2O (932.8 eV) [42]. The presence of copper carbonate was evidenced by the presence of the corresponding $CuCO_3$ component in the C 1 s spectra, found at about 288.6 eV (not shown). Despite the different treatment of the samples, the only difference observed is that the intensity of the main CuO component of the CCTO RF-O_2 sample decreases slightly on the expense of the Cu_2O subpeak. While for the reference sample the Ca 2p spectra indicate a pure CuO phase (834.8 eV), the CCTO RF-O_2 and CCTO RF-N_2 samples display a second spin–orbit component, indicating the formation of a $CaSO_4$ phase [42], due to the presence of sulphur, detected on the surface, Fig. 4a. Also the chemical bonding environment of Ti has been modified upon changed deposition conditions. The fitted Ti 2p spectra, displayed in Fig. 4b, show for the reference sample a principal component at about 458.4 eV, related to the TiO_2 phase, and a small high energy subpeak at 459.3 eV. The origin of the Ti 2p sub-peak is not quite clear, but is most probably related to oxygen vacancies forming five-fold coordinated sites in the TiO_2 lattice [43]. This is supported by the disappearance of this component for the sample prepared in the O_2 atmosphere, while for the CCTO RF-N_2 film, grown in the reducing environment, an increase of this phase can be observed.

Figure 5 depicts the *I–V* curves of the CCTO film. Low leakage current density is another important consideration for memory device applications. A typical leakage current characteristic for CCTO thin film is given. The curve was recorded with a voltage step width of 0.1 V and elapsed time of 1.0 s for each voltage, here the measured logorithmic current density (log J) versus the voltage (V) is

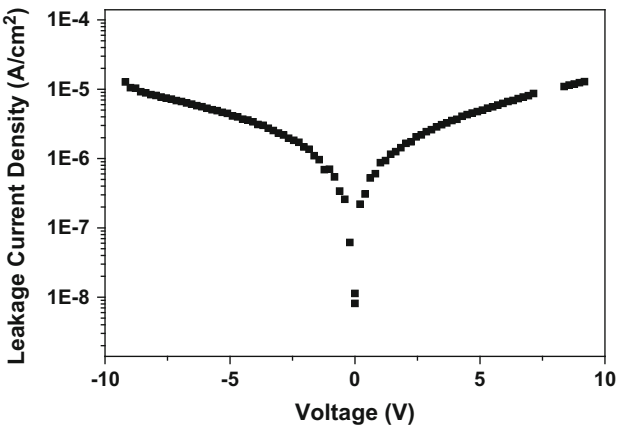

Fig. 5 Typical *I–V* hysteresis curve for the MFS structure for CCTO thin film deposited by the RF sputtering at room temperature and annealed at 600 °C for 2 h in a conventional furnace

shown. It can be seen that there are two clearly different regions. The current density increases linearly with the external electric field in the region of low electric field strengths, suggesting an ohmic conduction. This ohmic behaviour occurs in insulating film as long as the film is quase neutral, that is, as long as the bulk generated current in the film exceeds the current due to injected free carriers from the electrode. This current would be due to the hopping conduction mechanism in a low electric field, because thermal excitations of trapped electrons from one trap site to another dominate the transport in the films. At higher field strengths the current density increases exponentially, which implies that at least one part of the conductivity results from Schottky or Poole–Frenkel emission mechanism. The leakage current density at 1.0 V is equal to 10^{-7} A/cm^2. Since the conductivity is strongly affected by the characteristics of the film-electrode interface, the surface morphology of CCTO thin film is one of the major factors determining the leakage current in capacitors. The low leakage current value can be attributed to the small surface roughness as was observed by AFM in Fig. 3a. Chung et al., demonstrated the presence of electrical potential boundaries at CCTO grain boundaries and attributed the non-linear *I–V* curve to the grain boundary barrier layer. It was also proposed that the transport of charge inside grains has a linear relation, and the nonlinear curve is resulted from grain boundaries serving as a barrier to the carriers [44]. As shown in Fig. 3, CCTO films exhibit larger grain size which suggests more contribution from intra-grain transport.

It is well known that in most dielectric materials, the dielectric loss and leakage current density are related to the free carriers. The dielectric loss comes from two mechanisms [45–47]: the resistive loss and the relaxation loss of the dipole. In the resistive loss mechanism, the energy is consumed by free carriers in the film; while in the case of the relaxation loss mechanism, it is the relaxation of the dipole that expends energy. If there are free carriers in the films, the resistive loss is the dominant mechanism. Figure 6a shows the variation of dielectric permittivity and dielectric loss as a function of frequency for the CCTO film. At 1 kHz, the dielectric permittivity and dielectric loss for the capacitor, was 70 and 0.031, respectively. This value is quite low from that of the crystal, which is about 100 [3]. The large dielectric permittivity of CCTO has been interpreted as an extrinsic mechanism, which was assumed to come from the sample microstructure such as boundary or interface effects [38]. In fact, one recent paper has claimed that CCTO is a one-step internal barrier layer capacitor [5]. With such a model, one would conclude that the thin films have less defects than the crystals because of their lower dielectric permittivity. This is a possibility though it can often be the reverse. Thin films, with their

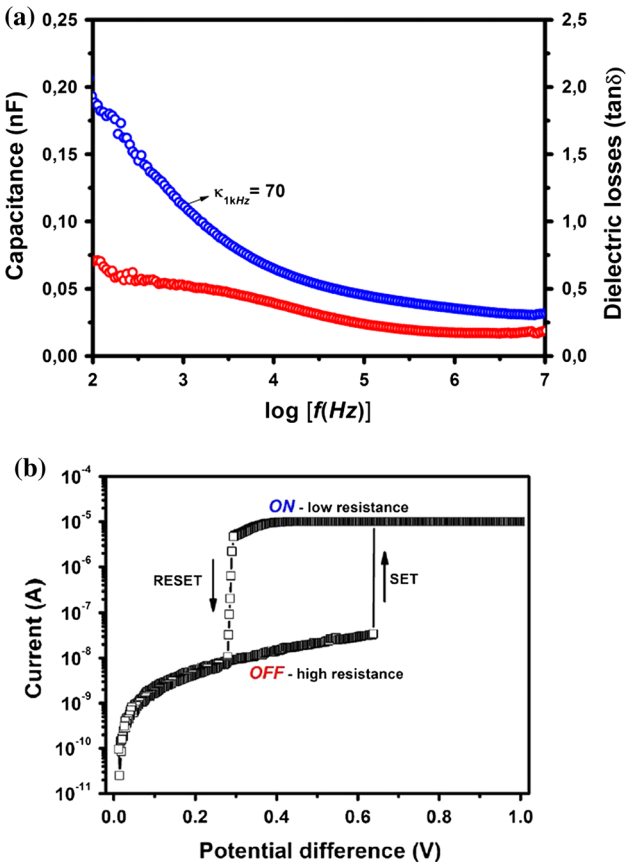

Fig. 6 **a** Variations of capacitance and dielectric losses versus frequency for CCTO film deposited by RF sputtering at room temperature and annealed at 600 °C for 2 h in a conventional furnace and **b** *I–V* characteristics of CCTO as-deposited in the set and reset modes

much reduced size in one dimension, may have less planar defects, such as grain boundaries and twin interfaces, than crystals, particularly if the latter have a large amount of intrinsic planar defects. Finally, it is worth pointing out that the dielectric loss in the thin film is actually lower than in the crystal. This may well be a reflection that the crystals have more defects than the thin films being the dielectric permittivity in the thin film ($\sim$70) much lower than in the crystal ($\geq$10,000). As it can be seen, the dielectric permittivity shows very little dispersion with frequency indicating that the films possess low defect concentrations at the interface film-substrate. The low dispersion of the dielectric permittivity and the absence of any relaxation peak in tan δ indicate that an interfacial polarization of the Maxwell–Wagner type and an interfacial polarization arisen from the electrode barrier are negligible in the film. The dielectric properties of the film obtained in the present work is comparable with that reported for polycrystalline CCTO thin films [8, 10, 39]. Dielectric permittivity as high as 2000 and dielectric loss of 0.05 has been reported for a polycrystalline CCTO thin film having 480 nm thickness

produced by PLD [10]. Such improvement may be a result of the closer package of uniform grains, crystal orientation and presence of buffer layer. Other explanation can be the presence of CuO based liquid phase sintering which increase the degree of disorder in the network forming positions with octahedral TiO_6 structural units. Such structural units may increase the rigidity of the network and cause to increase the values of dielectric parameters, as observed. The capability of storing multiple levels in one storage element is another important criterion in accessing emerging memory technologies. The current–voltage measurements were conducted on MFS capacitors to analyze the nature of the CCTO/Pt interface. Figure 6b shows a typical *I–V* hysteresis curve for the capacitor with polycrystalline nature. The *I–V* measurements were conducted by applying a small ac signal of 10 mV amplitude and 100 kHz frequency while the dc voltage was swept from a set and reset states. The curve clearly shows the regions of accumulation, depletion, and inversion, and the clockwise direction of the curve reveals that the MFS capacitor structure had a good dielectric polarization switching property. The injection type on/off switching behavior or the dielectric polarization switching behavior can be established by the round trip direction of the hysteresis loop of the current voltage response. A clockwise rotation in the *I–V* characteristic of a dielectric film on *p*-type Pt is expected when charge compensation on the surface is induced by the polarization present in the film. This mode of switching is the desired mode for memory operation. An accumulation layer appeared at negative bias voltages since the dielectric film was deposited on *p*-type substrate. The flat band voltage was slightly shifted toward positive voltage, which may be due to built-in immobile charges associated with ionic defects in the dielectric thin film. As the applied voltage was increased and became positive, a depletion layer was formed inside platinum near the interface. A further increase in voltage caused inversion of the surface. No significant difference in leakage currents was observed when the bias was reversed. This is reasonable because the capacitor system is completely symmetrical, and CCTO do not show evidence of ferroelectric behavior. Thus, applying voltage in direction or the other will be totally equivalent, regardless of whether the conduction is limited by interfacial barriers or by bulk-like mechanisms.

4 Conclusions

Good quality polycrystalline CCTO thin films was prepared by the RF sputtering on $Pt/Ti/SiO_2/Si$ (100) substrates at a room temperature followed by annealing at 600 °C for 2 h in a conventional furnace. Rietveld analysis revealed the polycrystalline nature of the film belonging to the *Im*-3 space group. The film shows good adhesion to the substrate and consist of homogeneous and crack-free microstructures formed of interconnected nanoparticles. The quantitative analysis obtained by XPS spectroscopy provided differences in the bonding structure and composition of the near surface region of the material annealed in oxygen and nitrogen atmospheres. The room temperature dielectric constant of the 600-nm-thick CCTO films annealed at 600 °C at 1 kHz was found to be 70. The leakage current of the MFS capacitor structure was governed by the Schottky barrier conduction mechanism and the leakage current density was lower than 10^{-7} A/cm^2 at 1.0 V. Leakage measurements don't show any evidence of ferroelectric behavior, regardless of whether the conduction is limited by interfacial barriers or by bulk-like mechanisms. Looking into the future, further improvement of the device structure will include the addition of a bottom metal layer to reduce potential series resistance problem in large scale and textured the films growth.

Acknowledgments The authors thank the financial support of the Brazilian research financing institutions: FAPESP.

References

1. M.A. Subramanian, D. Li, N. Duan, B.A. Reisner, A.W. Sleight, High dielectric constant in $ACu_3Ti_4O_{12}$ and $ACu_3Ti_3FeO_{12}$ phases. J. Solid State Chem. **151**(2), 323–325 (2000)
2. D. Szwagierczak, J. Kulawik, Dielectric properties of high permittivity ceramics based on $Dy_{2/3}CuTa_4O_{12}$. J. Alloys Compd. **491**(1–2), 465–471 (2010)
3. C.M. Wang, L. Shih-Yuan, K.S. Kao, Y.C. Chen, S.C. Weng, Microstructural and electrical properties of $CaTiO_3$–$CaCu_3Ti_4O_{12}$ ceramics. J. Alloys Compd. **491**(1–2), 423–430 (2010)
4. L. Ramajo, R. Parra, J.A. Varela, M.M. Reboredo, M.A. Ramirez, M.S. Castro, Influence of vanadium on electrical and microstructural properties of $CaCu_3Ti_4O_{12}$/$CaTiO_3$. J. Alloys Compd. **497**(1–2), 349–353 (2010)
5. R. Parra, R. Savu, L.A. Ramajo, M.A. Ponce, J.A. Varela, M.S. Castro, P.R. Bueno, E. Joanni, Sol–gel synthesis of mesoporous $CaCu_3Ti_4O_{12}$ thin films and their gas sensing response. J. Solid State Chem. **183**, 1209–1214 (2010)
6. A.G. Pinheiro, F.M.M. Pereira, M.R.P. Santos, Electric properties of $Bi_4Ti_3O_{12}$(BIT)-$CaCu_3Ti_4O_{12}$ (CCTO) composite substrates for high dielectric constant devices. J. Mater. Sci. **42**(6), 2112–2120 (2007)
7. R.S. de Figueiredo, A. Messai, A.C. Hernandes, A.S.B. Sombra, $BaTiO_3$ (BTO)–$CaCu_3Ti_4O_{12}$ (CCTO) substrates for microwave devices and antennas. J. Mater. Sci. **41**, 4623–4631 (1998)
8. W. Lu, L. Feng, G. Cao, Z. Jiao, Preparation of $CaCu_3Ti_4O_{12}$ thin films by chemical solution deposition. J. Mater. Sci. **39**, 3523–3524 (2004)
9. H. Wang, S. Li, J. He, C. Lin, Dielectric properties of $CaCu_3Ti_4O_{12}$ ceramics: effect of high purity nanometric powders. J Mater Sci Mater Electron **25**, 1842–1847 (2014)
10. M.J. Pan, B.A. Bender, A bimodal grain size model for predicting the dielectric constant of calcium copper titanate ceramics. J. Am. Ceram. Soc. **88**(9), 2611–2614 (2005)

11. L. Fang, M. Shen, W. Cao, Effects of post anneal conditions on the dielectric properties of $CaCu_3Ti_4O_{12}$ thin films prepared on Pt/Ti/SiO_2/Si substrates. J. Appl. Phys. **95**(11), 6483–6485 (2004)
12. L. Wu, Y. Zhu, S. Park, S. Shapiro, G. Shirane, Defect structure of the high-dielectric-constant perovskite $CaCu_3Ti_4O_{12}$. Phys. Rev. B **71**(1), 014118–014125 (2005)
13. V. Brizé, G. Gruener, J. Wolfman, K. Fatyeyeva, M. Tabellout, M. Gervais, Grain size effects on the dielectric constant of $CaCu_3Ti_4O_{12}$ ceramics. Mater. Sci. Eng. B **129**(1–3), 135–138 (2006)
14. P. Leret, J.F. Fernandez, J. Frutos, D. Fernandez-Hevia, Nonlinear I–V electrical behaviour of doped $CaCu_3Ti_4O_{12}$ceramics. J. Eur. Ceram. Soc. **27**(13–15), 3901–3905 (2007)
15. S.Y. Chung, I.D. Kim, S.J.L. Kang, Strong nonlinear current–voltage behaviour in perovskite-derivative calcium copper titanate. Nat. Mater. **3**, 774–778 (2004)
16. L. Chen, C.L. Chen, Y. Lin, Y.B. Chen, X.H. Chen, R.P. Bontchev, C.Y. Park, A. Jacobson, High temperature electrical properties of highly epitaxial $CaCu_3Ti_4O_{12}$ thin films on (001) $LaAlO_3$ Appl. Phys. Lett. **82**(14), 2317–2319 (2003)
17. A. Rothschild, H.L. Tuller, Gas sensors: new materials and processing approaches. J. Electroceram. **17**(2–4), 1005–1012 (2006)
18. I.D. Kim, A. Rothschild, T. Hyodo, H.L. Tuller, Microsphere templating as means of enhancing surface activity and gas sensitivity of CaCu3Ti4O12 thin films. Nano Lett. **6**(2), 193–198 (2006)
19. R. Savu, J.A. Varela, M.S. Castro, P.R. Bueno, Joanni E (2008) p-type semiconducting gas sensing behavior of nanoporous rf sputtered $CaCu_3Ti_4O_{12}$ thin films. Appl. Phys. Lett. **92**, 132110–132112 (2008)
20. R.A. Young, A. Sakthivel, T.S. Moss, C.O. Paiva-Santos, DBWS-9411-an upgrade of the DBWS*.* programs for Rietveld refinement with PC and mainframe computers. J. Appl. Cryst. **28**, 366–367 (1995)
21. Z. Li, H. Fan, Structure and electric properties of sol–gel derived $CaCu_3Ti_4O_{12}$ ceramics as a pyroelectric sensor. Solid State Ion. **192**(1), 682–687 (2011)
22. G. Zang, J. Zhang, P. Zheng, J. Wang, C. Wang, Grain boundary effect on the dielectric properties of $CaCu_3Ti_4O_{12}$ ceramics. J. Phys. D Appl. Phys. **38**, 1824–1827 (2005)
23. T. Li, R. Xue, J. Hao, Y. Xue, Z. Chen, The effect of calcining temperatures on the phase purity and electric properties of $CaCu_3Ti_4O_{12}$ ceramics. J. Alloys Compd. **509**, 1025–1028 (2011)
24. P. Lunkenheimer, R. Fichtl, S.G. Ebbiinghaus, A. Loidl, Nonintrinsic origin of the colossal dielectric constants in $CaCu_3Ti_4O_{12}$. Phys. Rev. B **70**, 172102–172106 (2004)
25. S. Krohns, P. Lunkenheimer, R. Fichtl, S.G. Ebbiinghaus, A. Loidl, Broadband dielectric spectroscopy on single-crystalline and ceramic $CaCu_3Ti_4O_{12}$. Appl. Phys. Lett. **91**, 022910–022912 (2007)
26. L. Fang, M. Shen, F. Zheng, Z. Li, J. Yang, Dielectric responses and multirelaxation behaviors of pure and doped $CaCu_3Ti_4O_{12}$ ceramics. J. Appl. Phys. **104**, 064110–064115 (2008)
27. C.M. Wang, K.S. Kao, S.Y. Lin, Y.C. Chen, S.C. Weng, Processing and properties of $CaCu_3Ti_4O_{12}$ ceramics. J. Phys. Chem. Solids **69**, 608–610 (2008)
28. L. Liu, H. Fan, P. Fang, Sol–gel derived $CaCu_3Ti_4O_{12}$ ceramics: synthesis, characterization and electrical properties. Mater. Res. Bull. **43**, 1800–1807 (2008)
29. H. Yu, H. Liu, D. Luo, M. Cao, Microwave synthesis of high dielectric constant $CaCu_3Ti_4O_{12}$. J. Mater. Process. Technol. **208**, 145–148 (2008)
30. A.F.L. Almeida, P.B.A. Fechine, M.P.F. Graça, A.S.B. Sombra, Structural and electrical study of $CaCu_3Ti_4O_{12}$ (CCTO) obtained in a new ceramic procedure. J. Mater. Sci. Mater. Electron. **20**, 163–170 (2009)
31. S.K. Jo, Y.H. Han, Sintering behavior and dielectric properties of polycrystalline $CaCu_3Ti_4O_{12}$. J. Mater. Sci. Mater Electron. **20**, 680–684 (2009)
32. S. Kwon, C.C. Huang, M.A. Subramanian, D.P. Cann, Effects of cation stoichiometry on the dielectric properties of $CaCu_3Ti_4O_{12}$. J. Alloys Compd. **473**, 433–436 (2009)
33. C.M. Wang, S.Y. Lin, K.S. Kao, Y.C. Chen, S.C. Weng, Microstructural and electrical properties of $CaTiO_3$–$CaCu_3Ti_4O_{12}$ ceramics. J. Alloys Compd. **491**, 423–430 (2010)
34. T.B. Adams, D.C. Sinclair, A.R. West, Giant barrier capacitance effects in $CaCu_3Ti_4O_{12}$. ceramics. Adv. Mater. **35**, 1321–1323 (2002)
35. D.C. Sinclair, T.B. Adams, F.D. Morrison, A.R. West, $CaCu_3Ti_4O_{12}$: one-step internal barrier layer capacitor. Appl. Phys. Lett. **80**, 2153–2155 (2002)
36. B.A. Bender, M.J. Pan, The effect of processing on the giant dielectric properties of $CaCu_3Ti_4O_{12}$. Mater. Sci. Eng. B **117**, 339–347 (2005)
37. L. Ni, X.M. Chen, X.Q. Liu, R.Z. Hhou, Microstucture-dependent giant dielectric response in $CaCu_3Ti_4O_{12}$ ceramics. Solid State Commun. **139**, 45–50 (2006)
38. P. Thomas, K. Dwarakanath, K.B.R. Varma, T.R.N. Kutty, Nanoparticles of the giant dielectric material, $CaCu_3Ti_4O_{12}$ from a precursor route. J. Phys. Chem. Solids **69**, 2594–2604 (2008)
39. B. Zhu, Z. Wang, Y. Zhang, Z. Yu, R. Xiong, Low temperature fabrication of the giant dielectric material $CaCu_3Ti_4O_{12}$ by oxalate coprecipitation method. Mater. Chem. Phys. **113**, 746–748 (2009)
40. C. Masingboon, P. Thongbai, S. Maensiri, T. Yamwong, S. Seraphin, Synthesis and giant dielectric behavior of $CaCu_3Ti_4O_{12}$ ceramics prepared by polymerized complex method. Mater. Chem. Phys. **109**, 262–270 (2008)
41. S. Krohns, J. Lu, P. Lunkennheimer, F. Gervais, F. Porcher, A. Loidl, Correlations of structural, magnetic, and dielectric properties of undoped and doped $CaCu_3Ti_4O_{12}$. Eur. Phys. J. B **72**, 173–182 (2009)
42. J.F. Moulder, W.F. Stickle, P.E. Sobol, K.D. Bomben, *Handbook of X-ray Photoelectron Spectroscopy* (Perkin-Elmer Corporation, Eden Prairie, 1992)
43. P.R. Bueno, R. Tararam, P. Parra, E. Joanni, J.A. Varela, A polaronic stacking fault defect model for $CaCu_3Ti_4O_{12}$ material: an approach for the origin of the huge dielectric constant and semiconducting coexistent features. J. Phys. D Appl. Phys. **42**(5), 1–9 (2009)
44. S.Y. Chung, I.D. Kim, S.J. Kang, Effects of annealing temperature on the resistance switching behavior of $CaCu_3Ti_4O_{12}$ films. Nat. Mater. **3**, 774–778 (2004)
45. C.C. Homes, T. Vogt, S.M. Shapiro, A.P. Ramirez, Optical response of high-dielectric-constant perovskite-related oxide. Science **293**, 673–680 (2001)
46. Y. Huang, D. Shi, Y. Li, Q. Wang, L. Liu, L. Fang, Effect of holding time on the dielectric properties and non-ohmic behavior of $CaCu_3Ti_4O_{12}$ capacitor-varistors. J. Mater. Sci. Mater. Electron. **24**, 1994–1999 (2013)
47. T. Prasit, P. Bundit, Y. Teerapon, M. Santi, Current–voltage nonlinear and dielectric properties of $CaCu_3Ti_4O_{12}$ ceramics prepared by a simple thermal decomposition method. J. Mater. Sci. Mater. Electron. **23**, 795–801 (2012)